

Physics

Special Topic: Two-dimensional Materials and Devices

Two-dimensional material-assisted remote epitaxy and van der Waals epitaxy: a review

Zhetong Liu^{1,2,3}, Bingyao Liu^{1,2,3}, Zhaolong Chen^{2,4,5}, Shenyuan Yang^{6,7}, Zhiqiang Liu^{7,8,*},
Tongbo Wei^{7,8,*}, Peng Gao^{1,3,9,*} & Zhongfan Liu^{2,4,*}¹Electron Microscopy Laboratory, and International Center for Quantum Materials, School of Physics, Peking University, Beijing 100871, China;²Beijing Graphene Institute (BGI), Beijing 100095, China;³Academy for Advanced Interdisciplinary Studies, Peking University, Beijing 100871, China;⁴Center for Nanochemistry (CNC), Beijing Science and Engineering Center for Nanocarbons, Beijing National Laboratory for Molecular Sciences, College of Chemistry and Molecular Engineering, Peking University, Beijing 100871, China;⁵Institute for Functional Intelligent Materials, National University of Singapore, Singapore 117575, Singapore;⁶State Key Laboratory of Superlattices and Microstructures, Institute of Semiconductors, Chinese Academy of Sciences, Beijing 100083, China;⁷Center of Materials Science and Optoelectronics Engineering, University of Chinese Academy of Sciences, Beijing 100049, China;⁸Research and Development Center for Semiconductor Lighting Technology, Institute of Semiconductors, Chinese Academy of Sciences, Beijing 100083, China;⁹Collaborative Innovation Center of Quantum Matter, Beijing 100871, China*Corresponding authors (emails: pgao@pku.edu.cn (Peng Gao); zfliu@pku.edu.cn (Zhongfan Liu); lzq@semi.ac.cn (Zhiqiang Liu); tbwei@semi.ac.cn (Tongbo Wei))

Received 27 November 2022; Revised 23 February 2023; Accepted 10 March 2023; Published online 3 July 2023

Abstract: Heteroepitaxy can reduce the cost and widen the application range of semiconductor film synthesis and device fabrication. However, the lattice and thermal expansion coefficient mismatches between epilayers and substrates limit the improvement of crystal quality and device performance. Two-dimensional (2D) material-assisted heteroepitaxy offers an effective solution to these challenges. The weak interaction at the interface between films and substrates facilitates the subsequent exfoliation and transfer of epilayer for the fabrication of flexible or high-power electronics. Herein, we summarize the modes of 2D material-assisted epitaxy, which can be classified into remote epitaxy, pinhole epitaxy and van der Waals epitaxy based on the interfacial interaction between the epilayers and substrates. Furthermore, we discuss in detail the improved crystal quality and functional applications, such as flexible devices, wavelength-modulated optoelectronic devices, and thermal management in high-power devices. Moreover, we highlight the challenges and prospects of 2D material-assisted epitaxy, providing roadmaps for lateral research and semiconductor production.

Keywords: graphene, 2D materials, heteroepitaxy, remote epitaxy, pinhole epitaxy, van der Waals epitaxy

Introduction

Epitaxy is a crucial technique to obtain high-quality semiconductor films and can be divided into homo-

epitaxy and heteroepitaxy based on the crystal relationships between substrates and epilayers. Although homoepitaxy can yield higher-quality films, heteroepitaxy is more important in semiconductor manufacturing, because single-crystal substrates are generally extremely expensive. In general, heteroepitaxy is performed on single-crystal substrates with a strict lattice-match requirement [1,2]. However, the lattice mismatch between the epilayers and selected substrates remains inevitable, which deteriorates the epilayer quality and, thus, the performance of the fabricated device [3]. Furthermore, as the growth typically undergoes a significant variation in temperature, the thermal expansion coefficient mismatch also plays an important role in determining the epitaxy quality. Therefore, effectively mitigating the influence of lattice and thermal expansion coefficient mismatches remains a challenge for heteroepitaxy technologies. Moreover, owing to the strong bonding interaction between substrates and epitaxial membranes, the current exfoliation and transfer methods incur high costs and low yields. Luckily, the management of interfacial interactions using two-dimensional (2D) materials provides an effective approach for the exfoliation and transfer of epilayers to other substrates.

An effective solution to modulate the epitaxy is to introduce a 2D material as a buffer layer [4–7]. To date, numerous high-quality multifunctional membranes exhibiting low strain and dislocation density have been fabricated using 2D materials interlayer to obtain high-performance devices [8–11]. Based on the understanding of the characteristics of the existing epitaxy strategies, an appropriate scheme could be designed to obtain the desired epitaxial films. The weak van der Waals interaction in these 2D material-assisted epitaxial interfaces is also conducive to the exfoliation and transfer of epitaxial films to the desired substrates, which allows the reuse of expensive substrates, thereby reducing the production cost; moreover, versatile devices based on other appropriate substrates can be fabricated, which can help attain better performance for electronic, optoelectronic, and medical devices [12–15].

In this review, we provide a comprehensive guide to the 2D material-assisted epitaxy, particularly considering graphene as the prototype, initially focusing on the problems of conventional epitaxy. Furthermore, we discuss in detail the three types of 2D material-assisted epitaxy categorized based on different epitaxy mechanisms: remote epitaxy, pinhole epitaxy, and van der Waals epitaxy. Moreover, we highlight the application of 2D material-assisted epitaxy in electronic, optoelectronic, and thermoelectric devices, considering the advantages of the electrical, thermal, and mechanical properties of 2D materials. Finally, we discuss the current challenges and provide an outlook for the development of this advanced epitaxy. We hope this review can serve as a significant reference for selecting the most appropriate epitaxy strategy.

Challenges of conventional heteroepitaxy and solutions with the assistance of 2D materials

As shown in Figure 1A, owing to strong interactions at the interface (e.g., covalent and ionic bonds), the conventional heteroepitaxy of films on substrates exhibits numerous shortcomings, which arise from the large lattice and thermal expansion coefficient mismatches between substrates and epitaxial films, thereby leading to large crystal deformation and strain [16–18]. Thus, various crystalline defects, such as dislocations and grain boundaries, arise to release this strain, reducing the efficiency, reliability, and service life of the device. Moreover, it is crucial to exfoliate and transfer epitaxial films to other well conductive substrates for high-power devices or flexible substrates to overcome substrate limitations, such as poor thermal and electric

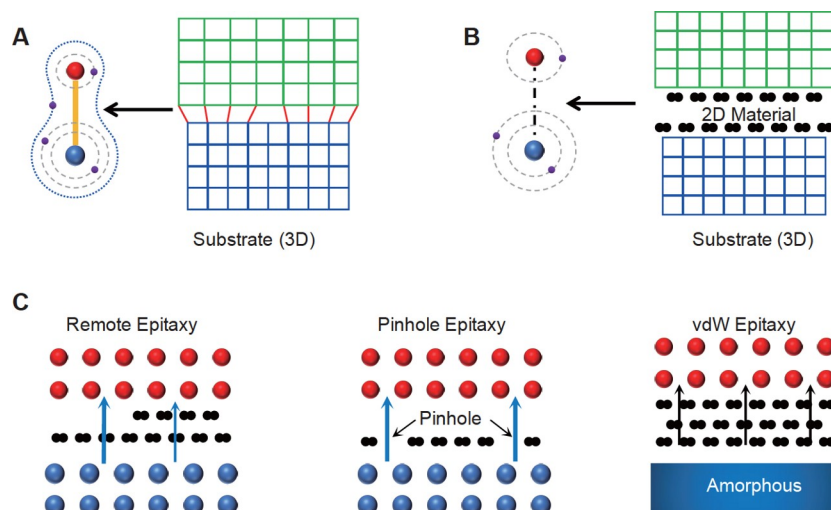


Figure 1 3D/3D and 3D/2D/3D structures and classification of 2D material-assisted epitaxy. Diagrams of interfacial structures of (A) conventional epitaxy (3D/3D) and (B) 2D material-assisted epitaxy (3D/2D/3D). (C) Schematics of three different types of 2D material-assisted epitaxy: remote, pinhole, and van der Waals epitaxy.

conductivities and rigid applications [19–22]. However, advanced technologies, such as sapphire-based laser stripping and silicon-based chemical etching, demonstrate a low yield and incur high costs. To overcome the existing challenges of conventional heteroepitaxy, novel epitaxial strategies are urgently required.

In recent years, the introduction of additional 2D materials (such as graphene [23–25] and hexagonal boron nitride [7,26–28]) has proven to be an effective solution to weaken the interfacial interactions; this approach benefits from the weak interaction nature of van der Waals bonding, as shown in Figure 1B. Herein, for the sake of clarity and simplification, we classified the 2D material-assisted epitaxy into three categories: remote epitaxy, pinhole epitaxy, and van der Waals epitaxy, as shown in Figure 1C.

Remote epitaxy refers to the utilization of few layers (typically less than three) of 2D materials as buffer layers to weaken but not completely shield the lattice potential of the substrate. There exist remote interactions at the interface owing to the penetration of substrate potential through the 2D material, which maintains the lattice guidance during epitaxy, and the weakened interactions between the substrate and epitaxial film provide the possibility for high-quality membranes with low strain and dislocation density. However, experimentally verifying the remote epitaxy mechanism still remains a challenge. Moreover, it is also difficult to precisely control the interfacial potential.

The oriented nucleation on 2D materials is sometimes suppressed owing to the lack of crystalline potentials from substrate and poor wettability. Pinhole epitaxy is a promising technique to promote nucleation, where the pinholes or defects in 2D materials can expose part of the substrate for adatoms to selectively nucleate at these sites and subsequently transversely coalesce into the film [29,30]. Such a pinhole can appear natively during the synthesis of 2D materials or be introduced through artificial treatment, including plasma or pre-growth annealing.

In van der Waals epitaxy, the 2D material completely screens the substrate potential and substitutes the role of the substrate such that the epitaxial layer nucleates and grows directly on the 2D material rather than the underlying substrate. Thus, it, along with the assistance of 2D material, can allow the epitaxy of films on any substrate regardless of the lattice limitations from substrates (even for amorphous ones).

In this review, we considered graphene as the prototype 2D material to describe the new growth modes and highlight the key progress. The graphene can either be grown directly on the substrate or be transferred externally. Notably, the nature of a 2D material also plays a crucial role in these epitaxy modes. For example, the liquid phase-exfoliated graphene or reduced graphene oxide (RGO) can be used as raw materials and subsequently coated on the substrate surface [31,32]. However, the graphene thus synthesized demonstrates an uneven number of layers, high defect density, and small domain size, which could degrade the quality of epitaxial films [33,34]. Moreover, graphene films can be grown on metal substrates via chemical vapor deposition (CVD) and further transferred to the substrate surface [6,35–37]. The quality of graphene synthesized using this technique is guaranteed; however, the time-consuming transfer process inevitably introduces damage, wrinkles, and metal or polymer residues. These problems may pose risks to the subsequent epitaxy, and thus, the performance of devices fabricated upon transferred graphene may be affected [38,39]. Moreover, when graphene is grown directly on the substrate via CVD, the problems associated with the coating or transfer process can be avoided. Furthermore, the application of CVD can simplify the fabrication process and thus reduce the involved costs [8,9,40–43].

Remote epitaxy

The concept of quasi-epitaxy was first proposed by So and Forrest *et al.* [44] in 1991, and remote epitaxy was recently reported by Kim *et al.* [7] in 2017. In the remote epitaxy, the introduction of 2D materials alters the substrate potential on the epilayers, which is an essential mechanism for single crystal growth. Under this scenario, the selection of 2D materials considering the nature and number of layers requires considerable attention (as shown in Figure 2A), which has a significant influence on the quality of the obtained epitaxial materials. Moreover, the selection strongly depends on the substrate and epilayers.

For example, the monolayer graphene generally cannot completely screen the strong potential fields of many substrates, which allows a remote interaction between epilayers and substrates [7]. Thus, various single-crystal materials prepared using different elements (such as GaAs, GaN, and LiF) can be grown on graphene-coated substrates by regulating the polarity and number of layers of 2D materials via homoepitaxy [45,46]. The transparency of 2D materials is controlled by their thickness and polarity. Owing to the severely dampened potential fluctuation as a result of the increased distance, as shown in Figure 2B [45], increasing the number of layers of graphene can effectively allow the screening of the field from the substrate. The three layers of graphene are sufficient to completely screen the GaN substrate potential during homoepitaxy [45]. Moreover, the residual potential of the substrate depends on the bond polarity arising from the difference in electronegativity between the bonding atoms, i.e., when the electronegativity is high, the bond polarity is high. Notably, both the 2D material and substrate polarity play crucial roles in controlling the interfacial interactions. The replacement of the nonpolar graphene with highly polar 2D materials (e.g., h-BN, MoS₂, and WS₂) can substantially attenuate the field penetration from the substrate. Meanwhile, the polarity of the 2D material gradually becomes dominating. For example, in the case of GaN homoepitaxy, the three layers of h-BN allow complete screening of the substrate potential and can determine the orientation of the as-grown GaN film, as shown in Figure 2C [45]. However, this case is no longer a case of remote epitaxy but a case of the van der Waals epitaxy mode, as discussed below.

Such a remote epitaxy strategy is even more useful in the case of large-mismatch heteroepitaxy [8,9,40,43]

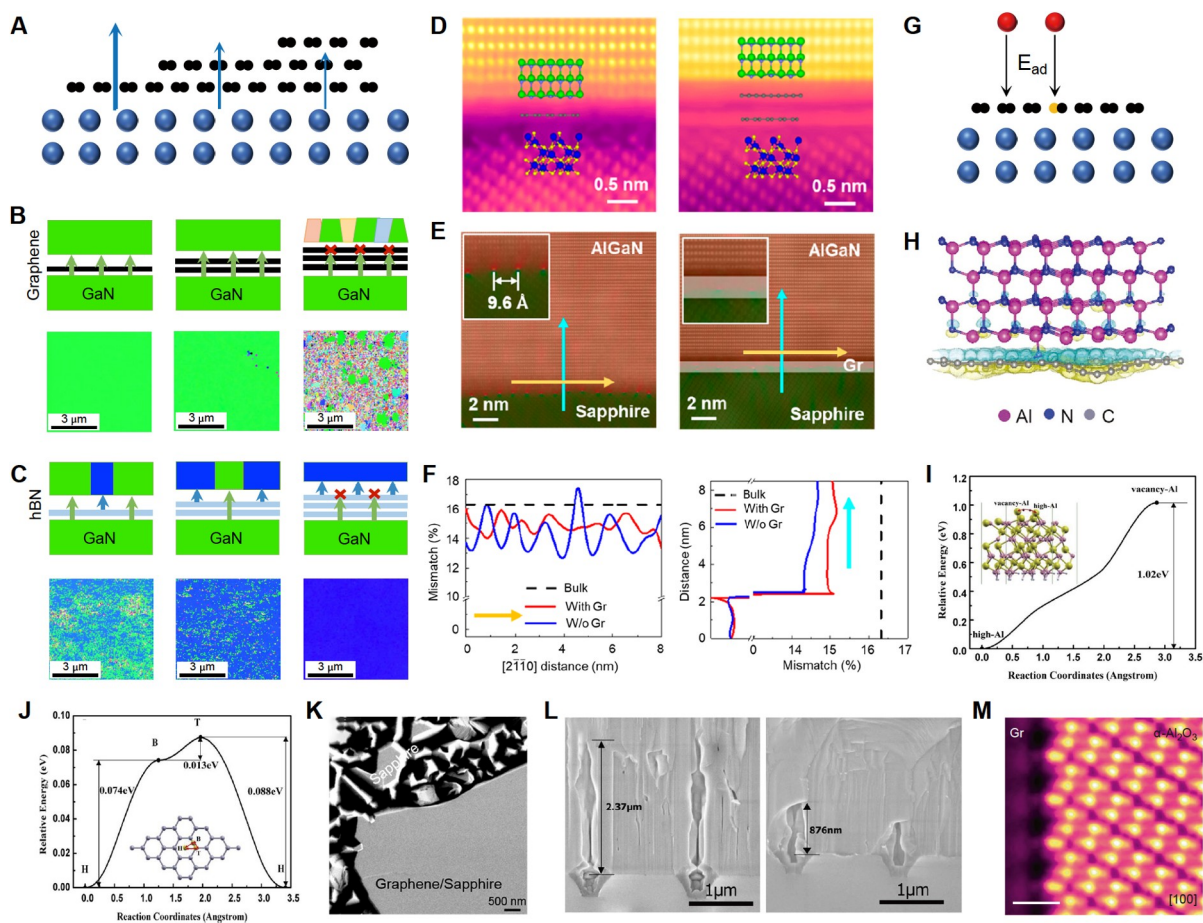


Figure 2 Remote epitaxy. (A) Schematic of the effect of the layer number of 2D materials on screening potential field from substrates. Comparison of the transparency of (B) graphene (Gr) and (C) h-BN with different layer numbers [45]. (D) High angle annular dark field scanning transmission electron microscopy (HAADF-STEM) images of the interfaces with monolayer and bilayer graphene [43]. (E) Geometric phase analysis e_{xx} mappings of the interface of AlGaN/sapphire without and with Gr [43]. (F) Fluctuation of in-plane lattice mismatch of nitride with respect to sapphire and in-plane lattice mismatch of strain-free AlGaN with respect to sapphire and AlGaN/sapphire without and with Gr, respectively [43]. (G) Schematic of the effects of 2D materials on nucleation and diffusion. E_{ad} , adsorption energy. (H) Diagram of the bonding of an Al adatom to pyrrolic N defect on graphene introduced by N_2 plasma treatment [9]. Diffusion barriers of Al adatoms (I) on sapphire substrate and (J) graphene across different adsorption sites [47]. (K) Scanning electron microscopy (SEM) image of the AlN domains on sapphire and Gr/sapphire, respectively [40]. (L) SEM images of AlN membranes on the nanopatterned sapphire substrate (NPSS) without and with Gr [47]. (M) HAADF-STEM image of the Gr/ Al_2O_3 interface [48]. The scale bar in (M) is 0.5 nm.

compared with that in homoepitaxy because the principle of remote epitaxy is to reduce the substrate potential, i.e., weaken the interaction. For a large-mismatch system, this strategy is expected to mitigate huge stress and reduce the high density of dislocations at the heterointerface, as shown in Figures 2D–2F [43]. With one or two layers of graphene as the buffer layer, the grown GaN on sapphire (with ~16% lattice mismatch) is obtained as a single-crystal substance. Graphene reduces the in-plane strain by 30% and suppresses the density of mismatch dislocations. The graphene-coated substrates also inhibit local lattice distortions near the steps on substrates. Consequently, the reduced in-plane compressive strain decreases the density of edge dislocations down to the same level as that of the screw ones [43].

Furthermore, we consider the nitride/graphene/sapphire system as an example to discuss the details of the nucleation and growth mechanism of remote epitaxy. First, as Figure 2G demonstrates, the epilayer nu-

creation is dependent on the adsorption energy (E_{ad}) of the precursor on different surfaces. AlN tends to nucleate on the bare sapphire substrate rather than on a dangling bond-free graphene surface; the E_{ad} of Al adatoms bonding to graphene can be increased from ~ 1.1 to 5.9–8.6 eV through nitrogen plasma treatment so as to introduce pyrrolic N into graphene, which shows an enhanced reactivity of graphene to nucleation. Thus, adatoms tend to nucleate at these sites, as shown in Figures 2G and 2H [9]. Further, compared with the bare sapphire substrate, graphene can reduce the migration barrier (Figures 2I and 2J [47]) and thus promote lateral epitaxy, thereby facilitating the rapid coalescence of the nitride film on graphene and the lateral overgrowth on the graphene-free region. Finally, a flat film is obtained (Figure 2K [40]). Therefore, the growth time of metal organic chemical vapor deposition (MOCVD) could be shortened, and the cost could be reduced, as shown in Figure 2L [47]. Moreover, as the interface is not necessarily a simple van der Waals interface in some cases where an interfacial C–O–Al bond is formed during growth, the actual mechanism may be more complex and needs further research (Figure 2M [48]).

The 2D materials used in remote epitaxy are not limited to graphene, and other 2D materials can also be used to synthesize high-quality epitaxial films [32]. For epitaxial materials other than nitrides, remote epitaxy can also be utilized for the growth of halide perovskite films with controllable dislocation density [49]. The previous studies on the growth of crystal materials by remote epitaxy are summarized in Table 1 [7–9,40,43,47,49–58].

The strength of interface interactions can be further tuned through the pinhole epitaxy mode, as shown in Figure 1C. For example, if the substrate lacks polarity, the potential field cannot penetrate even through a monolayer of graphene. In this case, larger size (nanoscale or even microscale) defects can be intentionally introduced to expose parts of the substrate surface. The total interface interaction can be tuned using the ratio of uncovered to covered areas. Since the adsorption energy on the bare substrate is higher than that of graphene without dangling bonds, the epilayers selectively nucleate on the bare substrate and then laterally epitaxially cross the 2D material region and finally coalesce into continuous films. Notably, the film remains a single crystal, as the lattice of the epilayer is still aligned by the single crystal substrate. Such larger size

Table 1 Related reports based on the method of remote epitaxy

Growth method	Substrate type	2D materials	Epitaxial layer	Exfoliation	Ref.
MOCVD	GaAs	Graphene	GaAs	Yes	[7]
MOCVD	Sapphire	Graphene	AlN	–	[8]
MOCVD	Sapphire	Graphene	AlGaN/AlN	–	[9]
MOCVD	Sapphire	Graphene	AlN	–	[40]
MOCVD	Sapphire	Graphene	GaN	–	[43]
MOCVD	Sapphire	Graphene	AlN	–	[47]
CVD	NaCl, CaF ₂	Graphene	CsPbBr ₃	Yes	[49]
MBE	Sapphire	Graphene	GaN	–	[50]
MBE	Sapphire	Graphene	GaN	–	[51]
MBE	Mo	MoS ₂	GaN	Yes	[52]
MBE	Sapphire	WSe ₂	GaN	–	[53]
MOCVD	Sapphire	Graphene	AlGaIn	–	[54]
MOVPE	Sapphire	Graphene	GaN	Yes	[55]
MOCVD	Sapphire	Graphene	AlN	–	[56]
MOCVD	Sapphire	Graphene	AlN	–	[57]
PLD and MBE	SrTiO ₃ , MgAl ₂ O ₄ , and Gd ₃ Ga ₅ O ₁₂	Graphene	SrTiO ₃ , CoFe ₂ O ₄ , and Y ₃ Fe ₅ O ₁₂	Yes	[58]

Table 2 Related reports based on the method of pinhole epitaxy

Growth method	Substrate type	2D materials	Epitaxial layer	Exfoliation	Ref.
CVD	Ge	Graphene	GaAs	–	[29]
MBE	Sapphire	Graphene	GdPtSb	Yes	[30]
MBE	GaSb	Graphene	GaSb	Yes	[59]
MOCVD	GaAs, Ge, and InAs	Graphene	GaAs, Ge, and InP	Yes	[60]

defects in 2D materials can be introduced by artificial treatment such as pre-growth annealing and patterning through lithography techniques [29,30]. Moreover, some pinholes are caused by native oxide desorption from substrates. Manzo *et al.* [59] reported that the lateral epitaxial growth of GaSb films on graphene/GaSb (001) can be achieved using ~10 and 300 nm pinhole defects in graphene as selective nucleation sites followed by epitaxial lateral overgrowth. Owing to the advantage of the pinhole mode that the interface interaction can be continuously controlled, pinhole mode can also support the opportunity for the exfoliation of the epilayers. For example, artificially-designed graphene nanopatterns can be introduced as a hetero-integration platform to fabricate freestanding membranes with fewer defects through pinhole epitaxy [60]. The previous studies on the growth of crystal materials by pinhole epitaxy are summarized in Table 2 [29,30,59,60].

Van der Waals epitaxy

The concept of van der Waals epitaxy was first proposed by Koma *et al.* [61,62] in 1984. The substrate potentials are completely shielded by the interlayer 2D materials, and the lattice of 2D materials instead acts as a template for the epilayers to nucleate. Accordingly, epitaxy growth can be achieved on arbitrary substrates (even amorphous without any lattice) with the help of appropriate 2D materials, which can help overcome the limitations arising from substrates (Figure 3A) [63]. However, the lattice mismatch between the target epilayers and 2D materials should be carefully considered. For example, for the hexagonal structure, either a direct match or a rotation match may work, as shown in Figure 3B. Such information requires careful analysis even when employing first-principles calculations. For van der Waals epitaxy, large-size single-crystal 2D layers are generally required to align the orientation of nuclei. Thus, the transferred 2D materials from metal substrates are preferred. As the lattice alignment is solely determined by 2D materials, the stronger the polarity of 2D materials, the easier it is to produce a satisfactory induction effect for epitaxy [6,45,64].

Chung *et al.* [4] achieved the heteroepitaxy of GaN films with aligned out-of-layer directions on thick graphene-layered sheets (Figure 3C). However, the in-plane direction is even more challenging to control. As shown in Figures 3D–3H, using the large-size single-crystal monolayer graphene, nearly single-crystal GaN films with limited in-plane orientations were obtained on Gr/glass substrate. The results demonstrate that the preferred in-plane rotation angles of nitride grains on graphene are 0°, 10.9°, and 30°, respectively [65]. Additionally, single-crystal GaN films can be obtained on SiO₂/Si(100) substrate [66]. This can be explained by considering the lattice rotation during the epitaxy growth of nitrides; moreover, the lattice mismatch of transition metal dichalcogenide materials such as MoS₂ and WS₂ is much less than that of graphene and h-BN (Figure 3B). Thus, single-crystal nitride epilayers on the WS₂/glass substrate are further achieved, as shown in Figures 3I–3K [67–69]. The largest difference between remote epitaxy and van der Waals epitaxy arises

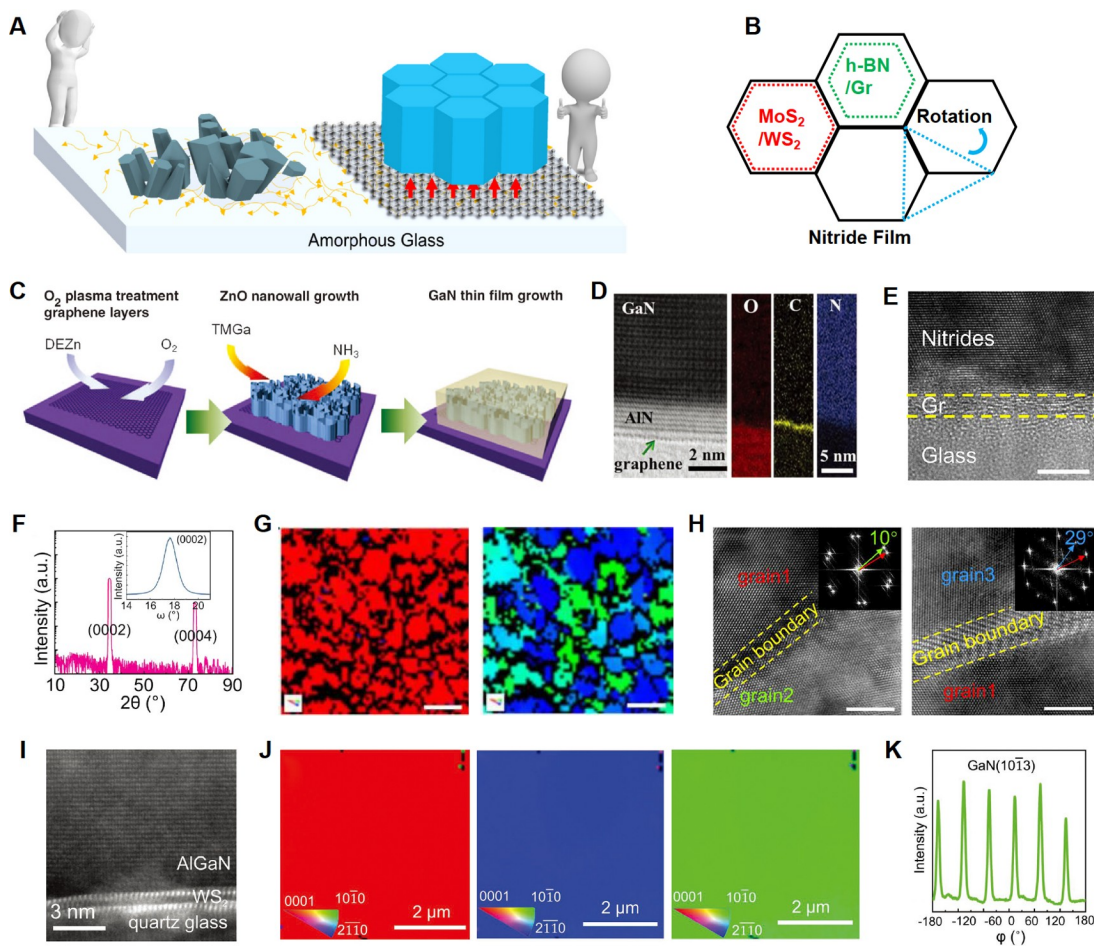


Figure 3 Van der Waals epitaxy. (A) Schematic of graphene lattice-guided nitride film growth on amorphous substrates [63]. (B) Schematic of lattice mismatches between MoS₂, WS₂, h-BN, and graphene (Gr) with nitrides and grain rotation in the in-plane direction. (C) Diagram of the fabrication process of GaN epitaxial film by introducing Gr layers and ZnO nanowall [4]. (D) HAADF-STEM image of the interface and electron energy loss spectroscopy mappings of O, C, and N elements at the interface [66]. (E) High-resolution transmission electron microscopy (HRTEM) image of the interface of nitrides/Gr/glass [65]. (F) X-ray diffraction (XRD)-2θ scan spectrum of GaN film [65]. (G) Electron backscatter diffraction (EBSD) inverse pole figure (IPF) images of GaN films grown on Gr/glass [65]. (H) HRTEM images of two GaN grains with 10° and 29° relative rotations, respectively [65]. (I) HAADF-STEM image of the interface by introducing WS₂ as a buffer layer [67]. (J) EBSD-IPF images of GaN films grown on WS₂/glass in the Z-, X-, and Y-directions [67]. (K) XRD-φ scan of GaN from a probed area of 1 mm × 10 mm [67]. The scale bars in (E), (G), (H), and (J) are 5 nm, 1 μm, 5 nm, and 2 μm, respectively.

from the origin of the epilayer lattice. In remote epitaxy, the epilayers are still guided by the substrate potential; in contrast, in van der Waals epitaxy, the epilayers demonstrate no interaction with the substrate. Therefore, the lattice mismatch between 2D materials and epilayers should be considered in van der Waals epitaxy, while that between substrates and epilayers should be considered in remote epitaxy. After the nucleation process, the lateral overgrowth and coalescence processes are similar in these two cases.

Besides the film growth, van der Waals epitaxy has also been widely used to grow nanostructures. For example, using graphene as a buffer layer, vertically aligned GaN nanorods with *c*-axis orientation can be obtained on graphene-covered Si(111) and Si(100) substrates [70]. Moreover, the application of van der Waals epitaxy is not limited to atomically thin 2D materials but also has been intensively reported for muscovite mica substrates, e.g., for the growth of ZnO nanowire arrays [71]. Some of the related reports on

Table 3 Related reports utilizing van der Waals epitaxy

Growth method	Substrate type	2D materials	Epitaxial layer	Exfoliation	Ref.
MOCVD	Sapphire	Graphene	GaN/ZnO	Yes	[4]
MOVPE	Sapphire	h-BN	AlGaIn, AlN	Yes	[5]
MOCVD	SiC	Graphene	GaN	Yes	[6]
MOCVD	Sapphire	Graphene	GaN/AlN	–	[37]
MOVPE	Sapphire	h-BN	AlN	Yes	[64]
MOCVD	Glass	Graphene	AlGaIn	Yes	[65]
MOCVD	SiO ₂ /Si	Graphene	GaN/AlN	–	[66]
MOCVD	Glass	WS ₂	GaN/AlGaIn	Yes	[67]
MOVPE	SiO ₂ /Si	WS ₂	GaN	Yes	[68]
MOVPE	SiO ₂ /Si	WS ₂	GaN	–	[69]
MOVPE	Si(100), Si(111)	Graphene	GaN	–	[70]
MOCVD	Sapphire	Graphene	GaN	–	[72]
MOCVD	SiO ₂	Graphene	GaN/AlGaIn	–	[73]
MOCVD	SiO ₂ /Si	Graphene	GaN	Yes	[74]
MOCVD	SiO ₂ /Si	Graphene	GaN/AlN	Yes	[75]
MOCVD	Glass	Graphene	GaN/AlN	–	[76]
MBE	Si(100)	Graphene	GaN	–	[77]
MBE	SiC(0001)	Graphene	GaN	–	[78]
MOCVD	Sapphire	Graphene	AlN	–	[79]

the growth of crystal materials by utilizing van der Waals epitaxy are summarized in Table 3 [4–6,37,64–79].

Furthermore, considering nitride growth as an example, the conventional epitaxy technology is relatively mature at present. On NPSSs, the dislocation density of AlN films grown by 2D material-assisted epitaxy (screw: $1.55 \times 10^8 \text{ cm}^{-2}$; edge: $2.60 \times 10^9 \text{ cm}^{-2}$) [47] remains higher than that of AlN films grown by conventional epitaxy (screw: $5.9 \times 10^7 \text{ cm}^{-2}$; edge: $2.3 \times 10^8 \text{ cm}^{-2}$) [80]. Therefore, there exists further scope for the improvement of the 2D material-assisted epitaxial growth, which is expected to be much better than conventional one.

Exfoliation, transfer progress and enabled flexible devices based on 2D material-assisted epitaxy

The weak van der Waals-interlayer interactions in 2D material-assisted epitaxy increase the ease of the epilayer exfoliation and transfer process compared with conventional epitaxy, which is a prominent advantage of 2D material-assisted epitaxy. A feasible stripping and transfer process is shown in Figure 4A. First, a metal (i.e., Ni) layer is deposited on the grown films. Second, a supporting layer of thermally releasable tape (TRT) is attached to the metal layer to assist in the peeling off of the epilayers from the substrate. Third, the TRT/metal/epilayer stack is transferred to another substrate, and the process is completed after the movement of the TRT and metal layer [60,81–83]. As shown in Figure 4B, the 2D material buffer layer weakens the interfacial interaction, which can be beneficial for exfoliation [7]. As elemental semiconductor substrates lack polarity, their potential cannot even penetrate a single layer of 2D materials. Luckily, pinhole epitaxy using nanopatterned graphene enables the exfoliation, as shown in Figure 4C [60]. In addition to these semiconductor thin films, freestanding single-crystal complex oxide films can be fabricated by remote epitaxy. Artificial heterostructures are further fabricated by directly stacking such films, which is not possible in the case of conventional methods (Figure 4D) [58].

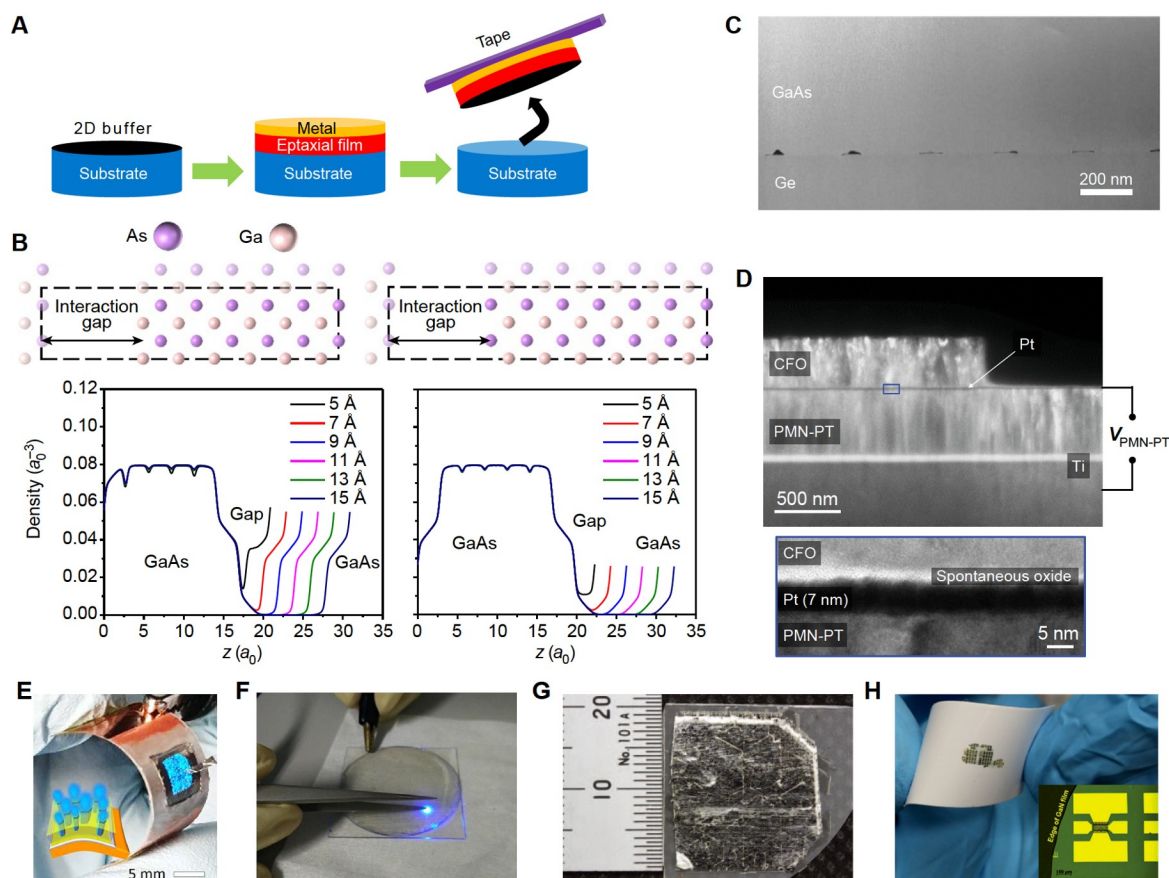


Figure 4 Technique of exfoliation and transfer based on 2D material-assisted epitaxy and related flexible devices. (A) Schematic of the transfer process based on 2D material. (B) Density functional theory calculation results of plane-averaged electron density of GaAs for As-Ga and As-As interactions [7]. (C) HAADF-STEM image of GaAs grown on patterned graphene/Ge [60]. (D) Transmission electron microscopy image of the heterostructure of $\text{CoFe}_2\text{O}_4/\text{Pb}(\text{Mg}_{1/3}\text{Nb}_{2/3})\text{O}_3\text{-PbTiO}_3$ film [58]. (E) Photograph and structure schematic of microrod LED [55]. (F) Image of the fabricated blue LED via van der Waals epitaxy [65]. (G) Photograph of the transferred nitride film on the sapphire substrate using an h-BN buffer layer [5]. (H) Image of flexible GaN HEMT devices [85].

The exfoliation method offers opportunities for the fabrication of flexible devices. Graphene enables device transfer and wafer reuse, which largely reduces the cost of some expensive single-crystal substrates. After exfoliation, the devices can be transferred onto other flexible substrates (Figure 4E) [55]. Moreover, van der Waals epitaxy overcomes the limitation of the requirement of single-crystal substrates. As shown in Figure 4F, a wafer-scale flexible GaN-based light-emitting diode (LED) with a high internal quantum efficiency on amorphous can be achieved by van der Waals epitaxy [65]. Recently, such 2D material-assisted epitaxy-enabled freestanding piezoelectric GaN membrane was successfully applied in chipless wireless electronic skin (e-skin), which can sense strain and ion concentrations in sweat and pulse monitoring [13,84].

Other than graphene, 2D material buffer layers, such as h-BN, can also be used for stripping and transferring epilayers or devices. As shown in Figure 4G, h-BN is used as a buffer layer for the growth of GaN film and provides a shear plane that enables the mechanical transfer of GaN-based devices to external substrates [5]. Additionally, a flexible GaN-based high electron mobility transistor (HEMT) radio-frequency device, whose superior performance is achieved by chemical-free transfer to flexible substrates, can be fabricated using an h-BN buffer layer, as shown in Figure 4H [85].

Other applications based on 2D material-assisted epitaxy

The 2D material-assisted epitaxy can also be used for several crucial applications in electronic, optoelectronic, and thermoelectric devices.

2D material-assisted epitaxy can modulate the performance of photoelectric devices by strain engineering. The large lattice and thermal expansion mismatches between the substrate and epitaxial film result in large strains and high dislocation density in the epitaxial layers in conventional epitaxy, which degrades the film quality and device efficiency. As shown in Figures 5A and 5B, the remaining strains in the epilayers are largely reduced because of the weakened epitaxial interaction by the insertion of a 2D material buffer layer [54]. This leads to a corresponding decrease in the dislocation density [57]. The low-strain semiconductor templates offer a suitable environment for alloys with atoms of different sizes, i.e., high-In-component multiple quantum wells (MQWs) can be realized [54]. The fabricated LEDs demonstrate long-range emission wavelengths, including yellow [43], green [50], cyan (Figure 5C) [54], blue [8], and ultraviolet (UV) [9,56,86].

The excellent thermal conductivity of graphene and h-BN may help solve the heat dissipation problems in high-power devices. Owing to the low thermal conductivity of conventional substrates, the problem of self-heating is severe for high-power optoelectronic devices and deteriorates the performance of devices. Thus, thermal management is critical to improving the efficiency and reliability of devices. By introducing fewer layers of graphene at the interface, the heat dissipation of GaN-based transistors can be significantly improved, and the lifetime of the device can be increased by an order of magnitude [87]. Moreover, patterned RGO can also be utilized to alleviate the self-heating problem of GaN-based LEDs through its heat dis-

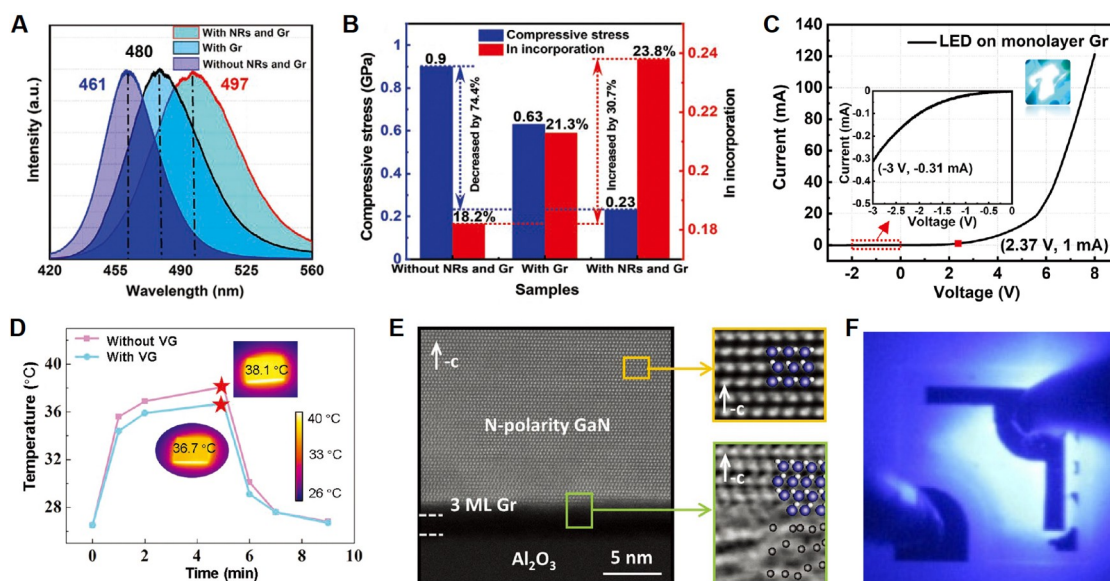


Figure 5 Other applications based on 2D material-assisted epitaxy. (A) Photoluminescence spectra of the MQWs on sapphire, with monolayer Gr, and with nanorods (NRs) and monolayer Gr [54]. (B) Histograms of compressive stress and In incorporation of different samples [54]. (C) *I-V* characteristic of cyan LED grown on graphene [54]. (D) Measured temperatures of AlN films on a sapphire substrate with and without vertical graphene (VG) [79]. (E) HAADF-STEM image and integrated differential phase contrast images of the interface atomic structure of the GaN film with N-polarity [51]. (F) Photograph of LED after applying current using graphene as a transparent conductive electrode [88].

sipation capability and the reduction of thermal boundary resistance [31]. Owing to the ultra-high in-plane thermal conductivity of graphene, the introduction of vertically oriented graphene into the epitaxial layer of LED can further improve the heat dissipation performance of LED devices, which provides a new possibility for the fabrication of high-power devices, as shown in Figure 5D [79].

The preparation of films with specific polarity is also required owing to the objective needs in some cases, which can be achieved by conducting other treatments on graphene to manipulate the interface atomic configuration. For instance, as shown in Figure 5E, conducting atomic oxygen pre-irradiation on three-layer graphene, gallium- and nitrogen-polarity GaN films can be obtained by developing C-O-N-Ga and C-O-Ga-N configurations at the interface, respectively [51].

Graphene can also act as transparent conductive electrodes owing to its excellent electrical conductivity (Figure 5F) [4,88,89]. Høiaas *et al.* [90] reported the growth of AlGaN nanocolumns on bilayer graphene using plasma-assisted molecular beam epitaxy (MBE). Using graphene as a transparent electrode, the light of the UV LED in a flip-chip configuration is emitted directly from the side of the amorphous silica glass.

Conclusions and outlook

The new technology of 2D material-assisted epitaxy has emerged as a crucial epitaxy method and is receiving widespread attention. The present review briefly introduces the opportunities of the 2D material-assisted epitaxy to overcome the challenges of conventional epitaxy. The mechanism and advantages of remote, pinhole, and van der Waals epitaxy are discussed. We further suggest a strategy to select the appropriate mode and 2D materials to achieve high-quality epilayers based on the nature and application needs of the target epilayers, as shown in Table 4. Most commonly, with the introduction of 2D materials, the strength of interface interaction between the epilayers and substrate becomes weaker, enabling low strain and low dislocation density. Further, the weak interaction in these van der Waals interfaces leads to the fabrication of flexible, wavelength-modulated photoelectric, and high-power devices.

However, the technology of 2D material-assisted epitaxy is not mature compared with conventional heteroepitaxy. There remain certain questions and challenges to be solved, some of which are listed below:

(i) The transfer process of 2D materials is generally required for the target substrates because the direct growth of 2D materials on these substrates remains challenging in most cases. However, the transfer process is unlikely to be compatible with the mature current semiconductor technologies, as this process generally introduces residues and severe discontinuities, which influence the quality of the epilayers and reduce the reliability of the devices. Therefore, a wafer-scale continuous and clean transfer method is required in the future.

(ii) For the substrates that enable the direct growth of 2D materials, another challenge is the growth of 2D

Table 4 Epitaxy strategy and 2D material selection based on different factors

Method	Substrate type	2D material layer number	Applications
Remote epitaxy	Crystal (strong polarity)	1–2	High-quality epilayers and flexible devices
Pinhole epitaxy	Crystal (weak polarity)	1–2	High-quality epilayers
Van der Waals epitaxy	Crystal and amorphous	≥ 3	Flexible devices

materials with single-crystal features and uniform thickness at the wafer scale. Corresponding specialized equipment and optimized growth conditions are also required to achieve mass and low-cost fabrication.

(iii) Benefiting from the 2D material-enabled exfoliation and transfer, various heterointegration exfoliation technologies have been developed. However, there remains a large gap for such technology to meet the requirements of mass production in the current integrated circuit (IC) industry. Moreover, stripping technology needs to be further developed, which needs to consider both the quality of devices and the yield of transferred devices.

In the meantime, there remain numerous new application opportunities in the future, including the following:

(i) As the heat dissipation of devices could be effectively alleviated using graphene and h-BN buffer layers, high-power devices may be feasible by simply introducing these 2D materials.

(ii) The growth of high-quality nitride films on Si(100), which is compatible with complementary metal-oxide-semiconductor technologies, offers the possibility to integrate photonic devices into Si-based ICs.

(iii) The transferability of epilayer grown on 2D materials provides exciting opportunities for flexible electronics, high-power HEMT and LEDs, and film bulk acoustic resonators.

(iv) In addition, the 3D/2D heterointegration allows the generation of new interfaces, which may exhibit novel optical, electrical, and thermal properties [91–94].

Overall, with the development of 2D material-assisted epitaxy and post transfer technologies, the application of epitaxial layers, which are not constrained by lattice mismatch, is approaching reality. Moreover, advances in heteroepitaxial technology can promote industrial innovation and upgrading, and reduce production costs. Accordingly, this approach will help realize the demand for wearable electronics, 5G, and the Internet of Things in the future. Moreover, we believe that based on 2D material-assisted epitaxy, increasing numbers of prospective innovations will emerge in electronic, optoelectric, and thermoelectric applications.

Funding

The work was supported by the National Key R&D Program of China (2019YFA0708200), the National Natural Science Foundation of China (T2188101, 52125307, 52021006 and 12074369), the “2011 Program” from the Peking-Tsinghua-IOP Collaborative Innovation Center of Quantum Matter, Youth Innovation Promotion Association, CAS, and the Youth Supporting Program of Institute of Semiconductors.

Author contributions

Z.T.L. drafted the manuscript with the assistance of B.Y.L. and Z.L.C. under the direction of P.G. and Z.F.L. All co-authors discussed and commented on the manuscript.

Conflict of interest

The authors declare no conflict of interest.

References

- 1 Chen Y, Hong S, Ko H, *et al.* Effects of an extremely thin buffer on heteroepitaxy with large lattice mismatch. *Appl Phys Lett* 2001; **78**: 3352–3354.
- 2 Matthews J, Blakeslee A. Defects in epitaxial multilayers. I. Misfit dislocations. *J Cryst Growth* 1974; **27**: 118–125.

- 3 Li G, Wang W, Yang W, *et al.* GaN-based light-emitting diodes on various substrates: a critical review. *Rep Prog Phys* 2016; **79**: 056501.
- 4 Chung K, Lee CH, Yi GC. Transferable GaN layers grown on ZnO-coated graphene layers for optoelectronic devices. *Science* 2010; **330**: 655–657.
- 5 Kobayashi Y, Kumakura K, Akasaka T, *et al.* Layered boron nitride as a release layer for mechanical transfer of GaN-based devices. *Nature* 2012; **484**: 223–227.
- 6 Kim J, Bayram C, Park H, *et al.* Principle of direct van der Waals epitaxy of single-crystalline films on epitaxial graphene. *Nat Commun* 2014; **5**: 4836.
- 7 Kim Y, Cruz SS, Lee K, *et al.* Remote epitaxy through graphene enables two-dimensional material-based layer transfer. *Nature* 2017; **544**: 340–343.
- 8 Chen Z, Zhang X, Dou Z, *et al.* High-brightness blue light-emitting diodes enabled by a directly grown graphene buffer layer. *Adv Mater* 2018; **30**: 1801608.
- 9 Chen Z, Liu Z, Wei T, *et al.* Improved epitaxy of AlN film for deep-ultraviolet light-emitting diodes enabled by graphene. *Adv Mater* 2019; **31**: 1807345.
- 10 Chen Z, Gao P, Liu Z. Graphene-based LED: from principle to devices. *Acta Physico-Chim Sin* 2020; **36**: 1907004.
- 11 Liang D, Wei T, Wang J, *et al.* Quasi van der Waals epitaxy nitride materials and devices on two dimension materials. *Nano Energy* 2020; **69**: 104463.
- 12 Wang S, Sun C, Shao Y, *et al.* Self-supporting GaN nanowires/graphite paper: novel high-performance flexible supercapacitor electrodes. *Small* 2017; **13**: 1603330.
- 13 Kim Y, Suh J, Shin J, *et al.* Chip-less wireless electronic skins by remote epitaxial freestanding compound semiconductors. *Science* 2022; **377**: 859–864.
- 14 Kum H, Lee D, Kong W, *et al.* Epitaxial growth and layer-transfer techniques for heterogeneous integration of materials for electronic and photonic devices. *Nat Electron* 2019; **2**: 439–450.
- 15 Bae SH, Kum H, Kong W, *et al.* Integration of bulk materials with two-dimensional materials for physical coupling and applications. *Nat Mater* 2019; **18**: 550–560.
- 16 Matthews J, Blakeslee A. Defects in epitaxial multilayers. I. Misfit dislocations. *J Cryst Growth* 1974; **27**: 118–125.
- 17 Morelli DT, Heremans JP, Slack GA. Estimation of the isotope effect on the lattice thermal conductivity of group IV and group III-V semiconductors. *Phys Rev B* 2002; **66**: 195304.
- 18 Narayan J. Recent progress in thin film epitaxy across the misfit scale (2011 Acta Gold Medal Paper). *Acta Mater* 2013; **61**: 2703–2724.
- 19 Motoki K, Okahisa T, Matsumoto N, *et al.* Preparation of large freestanding GaN substrates by hydride vapor phase epitaxy using GaAs as a starting substrate. *Jpn J Appl Phys* 2001; **40**: 140–143.
- 20 Rogers JA, Someya T, Huang Y. Materials and mechanics for stretchable electronics. *Science* 2010; **327**: 1603–1607.
- 21 Peng M, Liu Y, Yu A, *et al.* Flexible self-powered GaN ultraviolet photoswitch with piezo-phototronic effect enhanced on/off ratio. *ACS Nano* 2016; **10**: 1572–1579.
- 22 Chen J, Oh SK, Nabulsi N, *et al.* Biocompatible and sustainable power supply for self-powered wearable and implantable electronics using III-nitride thin-film-based flexible piezoelectric generator. *Nano Energy* 2019; **57**: 670–679.
- 23 Chen XD, Chen Z, Jiang WS, *et al.* Fast growth and broad applications of 25-inch uniform graphene glass. *Adv Mater* 2017; **29**: 1603428.
- 24 Soldano C, Mahmood A, Dujardin E. Production, properties and potential of graphene. *Carbon* 2010; **48**: 2127–2150.
- 25 Jo G, Choe M, Lee S, *et al.* The application of graphene as electrodes in electrical and optical devices. *Nanotechnology* 2012; **23**: 112001.
- 26 Petravic M, Peter R, Kavre I, *et al.* Decoration of nitrogen vacancies by oxygen atoms in boron nitride nanotubes. *Phys Chem Chem Phys* 2010; **12**: 15349–15353.
- 27 Lin Y, Connell JW. Advances in 2D boron nitride nanostructures: nanosheets, nanoribbons, nanomeshes, and hybrids

- with graphene. *Nanoscale* 2012; **4**: 6908–6939.
- 28 Zhang K, Feng Y, Wang F, *et al.* Two dimensional hexagonal boron nitride (2D-hBN): synthesis, properties and applications. *J Mater Chem C* 2017; **5**: 11992–12022.
- 29 Lim ZH, Manzo S, Strohbeen PJ, *et al.* Selective area epitaxy of GaAs films using patterned graphene on Ge. *Appl Phys Lett* 2022; **120**: 051603.
- 30 Du D, Jung T, Manzo S, *et al.* Controlling the balance between remote, pinhole, and van der Waals epitaxy of heusler films on graphene/sapphire. *Nano Lett.* 2022; **22**: 8647–8653.
- 31 Han N, Viet Cuong T, Han M, *et al.* Improved heat dissipation in gallium nitride light-emitting diodes with embedded graphene oxide pattern. *Nat Commun* 2013; **4**: 1452.
- 32 Zhang L, Li X, Shao Y, *et al.* Improving the quality of GaN crystals by using graphene or hexagonal boron nitride nanosheets substrate. *ACS Appl Mater Interfaces* 2015; **7**: 4504–4510.
- 33 Paton KR, Varrla E, Backes C, *et al.* Scalable production of large quantities of defect-free few-layer graphene by shear exfoliation in liquids. *Nat Mater* 2014; **13**: 624–630.
- 34 Chen XD, Liu ZB, Zheng CY, *et al.* High-quality and efficient transfer of large-area graphene films onto different substrates. *Carbon* 2013; **56**: 271–278.
- 35 Yoo H, Chung K, Choi YS, *et al.* Microstructures of GaN thin films grown on graphene layers. *Adv Mater* 2012; **24**: 515–518.
- 36 Yoo H, Chung K, In Park S, *et al.* Microstructural defects in GaN thin films grown on chemically vapor-deposited graphene layers. *Appl Phys Lett* 2013; **102**: 051908.
- 37 Li Y, Zhao Y, Wei T, *et al.* Van der Waals epitaxy of GaN-based light-emitting diodes on wet-transferred multilayer graphene film. *Jpn J Appl Phys* 2017; **56**: 085506.
- 38 Liang X, Sperling BA, Calizo I, *et al.* Toward clean and crackless transfer of graphene. *ACS Nano* 2011; **5**: 9144–9153.
- 39 Lin Y, Jin C, Lee J, *et al.* Clean transfer of graphene for isolation and suspension. *ACS Nano* 2011; **5**: 2362–2368.
- 40 Qi Y, Wang Y, Pang Z, *et al.* Fast growth of strain-free AlN on graphene-buffered sapphire. *J Am Chem Soc* 2018; **140**: 11935–11941.
- 41 Chen Z, Chang H, Cheng T, *et al.* Direct growth of nanopatterned graphene on sapphire and its application in light emitting diodes. *Adv Funct Mater* 2020; **30**: 2001483.
- 42 Chen Z, Xie C, Wang W, *et al.* Direct growth of wafer-scale highly oriented graphene on sapphire. *Sci Adv* 2021; **7**: eabk0115.
- 43 Liu B, Chen Q, Chen Z, *et al.* Atomic mechanism of strain alleviation and dislocation reduction in highly mismatched remote heteroepitaxy using a graphene interlayer. *Nano Lett* 2022; **22**: 3364–3371.
- 44 So F, Forrest S. Evidence for exciton confinement in crystalline organic multiple quantum wells. *Phys Rev Lett* 1991; **66**: 20.
- 45 Kong W, Li H, Qiao K, *et al.* Polarity governs atomic interaction through two-dimensional materials. *Nat Mater* 2018; **17**: 999–1004.
- 46 Kim H, Lu K, Liu Y, *et al.* Impact of 2D-3D heterointerface on remote epitaxial interaction through graphene. *ACS Nano* 2021; **15**: 10587–10596.
- 47 Chang H, Chen Z, Li W, *et al.* Graphene-assisted quasi-van der Waals epitaxy of AlN film for ultraviolet light emitting diodes on nano-patterned sapphire substrate. *Appl Phys Lett* 2019; **114**: 091107.
- 48 Dou Z, Chen Z, Li N, *et al.* Atomic mechanism of strong interactions at the graphene/sapphire interface. *Nat Commun* 2019; **10**: 5013.
- 49 Jiang J, Sun X, Chen X, *et al.* Carrier lifetime enhancement in halide perovskite via remote epitaxy. *Nat Commun* 2019; **10**: 4145.
- 50 Liu F, Zhang Z, Rong X, *et al.* Graphene-assisted epitaxy of nitrogen lattice polarity GaN films on non-polar sapphire substrates for green light emitting diodes. *Adv Funct Mater* 2020; **30**: 2001283.
- 51 Liu F, Wang T, Zhang Z, *et al.* Lattice polarity manipulation of quasi-vdW epitaxial GaN films on graphene through

- interface atomic configuration. *Adv Mater* 2022; **34**: 2106814.
- 52 Zhao C, Ng TK, Tseng CC, *et al.* InGaN/GaN nanowires epitaxy on large-area MoS₂ for high-performance light-emitters. *RSC Adv* 2017; **7**: 26665–26672.
- 53 Tangi M, Mishra P, Tseng CC, *et al.* Band alignment at GaN/single-layer WSe₂ interface. *ACS Appl Mater Interfaces* 2017; **9**: 9110–9117.
- 54 Zhang S, Liu B, Ren F, *et al.* Graphene-nanorod enhanced quasi-van der Waals epitaxy for high indium composition nitride films. *Small* 2021; **17**: 2100098.
- 55 Jeong J, Wang Q, Cha J, *et al.* Remote heteroepitaxy of GaN microrod heterostructures for deformable light-emitting diodes and wafer recycle. *Sci Adv* 2020; **6**: eaaz5180.
- 56 Chang H, Chen Z, Liu B, *et al.* Quasi-2D growth of aluminum nitride film on graphene for boosting deep ultraviolet light-emitting diodes. *Adv Sci* 2020; **7**: 2001272.
- 57 Chang H, Liu Z, Yang S, *et al.* Graphene-driving strain engineering to enable strain-free epitaxy of AlN film for deep ultraviolet light-emitting diode. *Light Sci Appl* 2022; **11**: 88.
- 58 Kum HS, Lee H, Kim S, *et al.* Heterogeneous integration of single-crystalline complex-oxide membranes. *Nature* 2020; **578**: 75–81.
- 59 Manzo S, Strohbeen PJ, Lim ZH, *et al.* Pinhole-seeded lateral epitaxy and exfoliation of GaSb films on graphene-terminated surfaces. *Nat Commun* 2022; **13**: 4014.
- 60 Kim H, Lee S, Shin J, *et al.* Graphene nanopattern as a universal epitaxy platform for single-crystal membrane production and defect reduction. *Nat Nanotechnol* 2022; **17**: 1054–1059.
- 61 Koma A, Sunouchi K, Miyajima T. Fabrication and characterization of heterostructures with subnanometer thickness. *MicroElectron Eng* 1984; **2**: 129–136.
- 62 Koma A, Sunouchi K, Miyajima T. Fabrication of ultrathin heterostructures with van der Waals epitaxy. *J Vacuum Sci Tech B: Microelectron Process Phenomena* 1985; **3**: 724.
- 63 Sealy C. Graphene lattice guides thin film nitride growth. *Nano Today* 2021; **40**: 101275.
- 64 Wu Q, Guo Y, Sundaram S, *et al.* Exfoliation of AlN film using two-dimensional multilayer hexagonal BN for deep-ultraviolet light-emitting diodes. *Appl Phys Express* 2019; **12**: 015505.
- 65 Ren F, Liu B, Chen Z, *et al.* Van der Waals epitaxy of nearly single-crystalline nitride films on amorphous graphene-glass wafer. *Sci Adv* 2021; **7**: eabf5011.
- 66 Feng Y, Yang X, Zhang Z, *et al.* Epitaxy of single-crystalline GaN film on CMOS-compatible Si(100) substrate buffered by graphene. *Adv Funct Mater* 2019; **29**: 1905056.
- 67 Yin Y, Liu B, Chen Q, *et al.* Continuous single-crystalline GaN film grown on WS₂-glass Wafer. *Small* 2022; **18**: e2202529.
- 68 Gupta P, Rahman AA, Subramanian S, *et al.* Layered transition metal dichalcogenides: promising near-lattice-matched substrates for GaN growth. *Sci Rep* 2016; **6**: 23708.
- 69 Hossain E, Rahman AA, Shah AP, *et al.* Large-area, thermally-sulfurized WS₂ thin films: control of growth direction and use as a substrate for GaN epitaxy. *Semicond Sci Technol* 2020; **35**: 035011.
- 70 Heilmann M, Munshi AM, Sarau G, *et al.* Vertically oriented growth of GaN nanorods on Si using graphene as an atomically thin buffer layer. *Nano Lett* 2016; **16**: 3524–3532.
- 71 Utama MIB, Belarre FJ, Magen C, *et al.* Incommensurate van der Waals epitaxy of nanowire arrays: a case study with ZnO on muscovite mica substrates. *Nano Lett* 2012; **12**: 2146–2152.
- 72 Mun DH, Bae H, Bae S, *et al.* Stress relaxation of GaN microstructures on a graphene-buffered Al₂O₃ substrate. *Phys Status Solidi RRL* 2014; **8**: 341–344.
- 73 Li T, Liu C, Zhang Z, *et al.* Understanding the growth mechanism of GaN epitaxial layers on mechanically exfoliated graphite. *Nanoscale Res Lett* 2018; **13**: 130.
- 74 Chung K, Yoo H, Hyun JK, *et al.* Flexible GaN light-emitting diodes using GaN microdisks epitaxial laterally overgrown on graphene dots. *Adv Mater* 2016; **28**: 7688–7694.

- 75 Chung K, Beak H, Tchoe Y, *et al.* Growth and characterizations of GaN micro-rods on graphene films for flexible light emitting diodes. *APL Mater* 2014; **2**: 092512.
- 76 Liudi Mulyo A, Rajpalke MK, Kuroe H, *et al.* Vertical GaN nanocolumns grown on graphene intermediated with a thin AlN buffer layer. *Nanotechnology* 2019; **30**: 015604.
- 77 Kumaresan V, Largeau L, Madouri A, *et al.* Epitaxy of GaN nanowires on graphene. *Nano Lett* 2016; **16**: 4895–4902.
- 78 Fernández-Garrido S, Ramsteiner M, Gao G, *et al.* Molecular beam epitaxy of GaN nanowires on epitaxial graphene. *Nano Lett* 2017; **17**: 5213–5221.
- 79 Ci H, Chang H, Wang R, *et al.* Enhancement of heat dissipation in ultraviolet light-emitting diodes by a vertically oriented graphene nanowall buffer layer. *Adv Mater* 2019; **31**: 1901624.
- 80 Long H, Dai J, Zhang Y, *et al.* High quality 10.6 μm AlN grown on pyramidal patterned sapphire substrate by MOCVD. *Appl Phys Lett* 2019; **114**: 042101.
- 81 Shim J, Bae S, Kong W, *et al.* Controlled crack propagation for atomic precision handling of wafer-scale two-dimensional materials. *Science* 2018; **362**: 665–670.
- 82 Qiao K, Liu Y, Kim C, *et al.* Graphene buffer layer on SiC as a release layer for high-quality freestanding semiconductor membranes. *Nano Lett* 2021; **21**: 4013–4020.
- 83 Bae SH, Lu K, Han Y, *et al.* Graphene-assisted spontaneous relaxation towards dislocation-free heteroepitaxy. *Nat Nanotechnol* 2020; **15**: 272–276.
- 84 Yeon H, Lee H, Kim Y, *et al.* Long-term reliable physical health monitoring by sweat pore-inspired perforated electronic skins. *Sci Adv* 2021; **7**: eabg8459.
- 85 Glavin NR, Chabak KD, Heller ER, *et al.* Flexible gallium nitride for high-performance, strainable radio-frequency devices. *Adv Mater* 2017; **29**: 1701838.
- 86 Jia Y, Ning J, Zhang J, *et al.* Transferable GaN enabled by selective nucleation of AlN on graphene for high-brightness violet light-emitting diodes. *Adv Opt Mater* 2019; **8**: 1901632.
- 87 Yan Z, Liu G, Khan JM, *et al.* Graphene quilts for thermal management of high-power GaN transistors. *Nat Commun* 2012; **3**: 827.
- 88 Jo G, Choe M, Cho CY, *et al.* Large-scale patterned multi-layer graphene films as transparent conducting electrodes for GaN light-emitting diodes. *Nanotechnology* 2010; **21**: 175201.
- 89 Kim KS, Zhao Y, Jang H, *et al.* Large-scale pattern growth of graphene films for stretchable transparent electrodes. *Nature* 2009; **457**: 706–710.
- 90 Høiaas IM, Liudi Mulyo A, Vullum PE, *et al.* GaN/AlGaIn nanocolumn ultraviolet light-emitting diode using double-layer graphene as substrate and transparent electrode. *Nano Lett* 2019; **19**: 1649–1658.
- 91 Konstantatos G, Badioli M, Gaudreau L, *et al.* Hybrid graphene-quantum dot phototransistors with ultrahigh gain. *Nat Nanotech* 2012; **7**: 363–368.
- 92 Huang B, Xiang H, Yu J, *et al.* Effective control of the charge and magnetic states of transition-metal atoms on single-layer boron nitride. *Phys Rev Lett* 2012; **108**: 206802.
- 93 Ruzmetov D, Zhang K, Stan G, *et al.* Vertical 2D/3D semiconductor heterostructures based on epitaxial molybdenum disulfide and gallium nitride. *ACS Nano* 2016; **10**: 3580–3588.
- 94 Al Balushi ZY, Wang K, Ghosh RK, *et al.* Two-dimensional gallium nitride realized via graphene encapsulation. *Nat Mater* 2016; **15**: 1166–1171.